Use of the FDTD Thin-Strut Formalism for Biomedical Telemetry Coil Designs

Stefan Schmidt, *Student Member, IEEE,* and Gianluca Lazzi, *Senior Member, IEEE*

***Abstract*—The finite-difference time-domain (FDTD) method extended by thin-strut formalism was used to study the current coupling between rectangular coils for use in biomedical telemetry links. Further, a new stability condition, different from the Courant–Friedrichs–Lewy stability limit, was derived for the thin-strut method. Results obtained for varying coil sizes and distances of separation show that the thin-strut FDTD formulation, applied to the calculation of current coupling between telemetry coils, is in closer agreement to the analytical approximation than is the standard FDTD code. These results indicate that the thin-strut method is a promising method for the study and the design of coils for telemetry links between implantable and external devices.**

***Index Terms*—Biomedical telemetry, coils, electromagnetic coupling, finite-difference time-domain (FDTD) methods, numerical stability, thin-strut formulation.**

I. Introduction

In a wide range of biomedical applications, the power to energize an implanted device is provided from outside the body by inductive coupling, thus allowing power to be transmitted transcutaneously. This type of inductive coupling is advantageous because it avoids the undesirable surgical replacement of implanted power sources and the possibility of infection where wires would pierce the skin. Furthermore, it allows the transcutaneous transmission of telemetry data to and from implanted systems. The operational principles of these systems are very similar to those of RF identification (RFID) tags [1]. Biomedical telemetry systems usually consist of an external primary coil and an implanted secondary coil, which are separated by a layer of skin and tissues. The magnetic link allows the transfer of energy and information through the biological tissue using frequencies generally lower than 10 MHz.

Due to skin mobility and variations in the thickness of subcutaneous fatty tissue, misalignment of the coils easily occurs, leading to a change of transmission characteristics. There have been several approaches to the analysis and design of inductively coupled transcutaneous links, with the goal of minimizing misalignment effects and maximizing the coupling efficiency [2]–[6]. However, these approaches rely mainly on steady-state circuit analyses, geometric considerations for coupling optimization [7], and validation through experiments. To our knowledge, few full-wave computational electromagnetic techniques, such as a two-dimensional finite-element method [8], have been developed for the analysis and design of coupled coils in transcutaneous telemetry applications.

The finite-difference time-domain (FDTD) method [9] is very attractive for the study of biomedical applications because of its ability to efficiently model inhomogeneous materials and irregular geometries. In the conventional FDTD method, wires are often modeled as perfect electric conductors by forcing all tangential electric-field components on the wire surfaces to zero. However, for wires with very small cross sections, a very fine mesh is also necessary for accurate modeling, but it is often prohibitive because of the large computational cost that accompanies a fine discretization.

Holland and Simpson first proposed the thin-strut formalism [10], a sub-cell model for thin straight wire elements embedded in the FDTD grid, for electromagnetic pulse (EMP) modeling. We use the FDTD method extended by the thin-strut formalism to model the current coupling in biomedical telemetry systems.

II. Thin-Strut FDTD Formulation

A. Governing Equations and Derivation of the Algorithm

Using the $D-H$-formulation of the FDTD method [11], we obtain the system of equations for the normalized time-dependent fields

$$\frac{\partial \mathbf{D}}{\partial t} = c_0(\nabla \times \mathbf{H} - \mathbf{J}) \tag{1}$$

$$\mathbf{E}(\omega) = \frac{\mathbf{D}(\omega)}{\varepsilon_r(\omega)} \tag{2}$$

$$\frac{\partial \mathbf{H}}{\partial t} = -c_0(\nabla \times \mathbf{E}). \tag{3}$$

In this formulation, the generic $D-E$ relationship in (2) is used to describe the dispersive dielectric properties of biological tissues. For simplicity, we assume a lossless dielectric with $\varepsilon_r(\omega) = \text{const.} = \varepsilon_r$ in this derivation. The system of equations then reduces to

$$\frac{\partial \mathbf{D}}{\partial t} = c_0(\nabla \times \mathbf{H} - \mathbf{J}) \tag{4}$$

$$\frac{\partial \mathbf{H}}{\partial t} = -\frac{c_0}{\varepsilon_r}(\nabla \times \mathbf{D}). \tag{5}$$

To derive a sub-cell model for thin wires, we follow the thin-strut formalism [10]. We assume a wire oriented in the z-direction and write the θ component of the curl equation for the H-field (5) in cylindrical coordinates as

$$\frac{\partial H_\theta}{\partial t} = \frac{c_0}{\varepsilon_r}\left[\frac{\partial D_z}{\partial r} - \frac{\partial D_r}{\partial z}\right]. \tag{6}$$

Manuscript received October 29, 2003; revised April 1, 2004. This work was supported by the National Science Foundation under CAREER Award ECS 0091599, and in part by the Office of Science (BER), U.S. Department of Energy under Grant DE-FG02-04ER63572.

The authors are with the Department of Electrical and Computer Engineering, North Carolina State University, Raleigh, NC 27606-7914 USA (e-mail: lazzi@ncsu.edu).

Digital Object Identifier 10.1109/TMTT.2004.832019

Assuming a quasi-static field approximation inside an FDTD cell, we use the approximations for the currents I_z and the charge Q per unit length on the wire

$$H_\theta(r) = \frac{I_z}{2\pi r} \text{ and } D_r(r) = \frac{Q}{2\pi r} \tag{7}$$

which leads to

$$\frac{1}{2\pi r}\frac{\partial I_z}{\partial t} = \frac{c_0}{\varepsilon_r}\left[\frac{\partial D_z}{\partial r} - \frac{1}{2\pi r}\frac{\partial Q}{\partial z}\right]. \tag{8}$$

Integrating from the wire surface r_0 outward to some radius r and using the boundary condition that the tangential fields are zero at the wire surface $D_z(r_0) = 0$, we obtain

$$\begin{aligned}\frac{c_0}{\varepsilon_r}\cdot D_z(r) &= \left[\frac{\partial I_z}{\partial t} + \frac{c_0}{\varepsilon_r}\cdot\frac{\partial Q}{\partial z}\right]\cdot\int_{r_0}^{r}\frac{1}{2\pi r}\,d\rho \\ &= \left[\frac{\partial I_z}{\partial t} + \frac{c_0}{\varepsilon_r}\cdot\frac{\partial Q}{\partial z}\right]\cdot\frac{\ln(r/r_0)}{2\pi}.\end{aligned} \tag{9}$$

Introducing an in-cell inductance per unit length

$$L(r) = \ln(r/r_0)\frac{1}{2\pi} \tag{10}$$

we obtain one governing equation for the wire model

$$\frac{\partial I_z}{\partial t} = \frac{c_0}{\varepsilon_r}\left(\frac{\langle D_z(R)\rangle}{\langle L(R)\rangle} - \frac{\partial Q}{\partial z}\right) \tag{11}$$

where $\langle D_z(R)\rangle$ and $\langle L(R)\rangle$ are the average values of the electric fields and inductance, respectively, inside the occupied FDTD cell. R is the radius of a disc that has a cross-sectional area equivalent to the area of the corresponding FDTD cell. Similarly, by writing down the r component of the curl equation for the D-field in (4), using the cylindrical field approximations in (7), and performing the integration, we obtain the second governing equation for the thin-strut formalism

$$\frac{\partial Q}{\partial t} = -c_0\frac{\partial I_z}{\partial z}. \tag{12}$$

The field (4) and (5) are coupled to the wire (11) and (12) by the electric field D_z and the current density $J_z = I_z/I_z A_{\text{cross}}$, where A_{cross} is the cross-sectional area of the occupied cell.

Using central finite differences for temporal and spatial derivatives, the wire equations (11) and (12) are discretized as

$$\begin{aligned}I_z\big|_k^{n+\frac{1}{2}} &= I_z\big|_k^{n-\frac{1}{2}} + \frac{c_0\Delta t}{\varepsilon_r L(R)}\cdot D_z\big|_k^n \\ &\quad - \frac{c_0\Delta t}{\Delta z}\left(Q\big|_{k+\frac{1}{2}}^n - Q\big|_{k-\frac{1}{2}}^n\right)\end{aligned} \tag{13}$$

$$Q\big|_{k+\frac{1}{2}}^{n+1} = Q\big|_{k+\frac{1}{2}}^n - \frac{c_0 t}{z}\left(I_z\big|_{k+1}^{n+\frac{1}{2}} - I_z\big|_k^{n+\frac{1}{2}}\right). \tag{14}$$

To complete the algorithm, the field equations (4) and (5) are discretized using second-order accurate central differences on the Yee grid [9], where $\mathbf{D}$ and $\mathbf{H}$ are staggered in space and time. Note that, I_z, J_z, and D_z are collocated spatially for a wire with a current I_z oriented along the z-direction, while the charges Q are in the same location as H_z. Moreover, if I_z and $\mathbf{H}$ are updated at the same time step $t_{n+(1/2)}$, then Q and $\mathbf{D}$ are updated a half time step later at t_{n+1}.

B. Approximation of the In-Cell Inductance

The in-cell inductance $\langle L(R)\rangle$, introduced in (11), depends on the radius and location of a wire inside an FDTD cell [10]. We consider a wire centered in an FDTD cell and collocated with the E_z-field components and approximate the equivalent radius R for the calculation of $\langle L(R)\rangle$ as that of a disc with the same area as the occupied cell. Therefore, for a uniform cell size ($\Delta x = \Delta y = \Delta z = h$), we have

$$R = \frac{h}{\sqrt{\pi}} \tag{15}$$

and obtain the average in-cell inductance

$$\langle L(R)\rangle = \frac{\int_0^{2\pi}\int_{r_0}^{R} rL(r)\,dr\,d\theta}{\int_0^{2\pi}\int_{r_0}^{R} r\,dr\,d\theta} = \frac{\left(\frac{\pi r_0^2}{h^2} - 1\right) - \ln\left(\frac{\pi r_0^2}{h^2}\right)}{4\pi\left(1 - \frac{\pi r_0^2}{h^2}\right)}. \tag{16}$$

C. Stability Analysis

The Courant–Friedrichs–Lewy (CFL) stability condition that applies to the conventional FDTD method is not a sufficient condition for stability of the sub-cell model of the thin-strut FDTD method. An attempt to derive a stability bound for the thin-strut method was previously made [12]; however, the criterion derived by Grando *et al.* is not a sufficient condition for the stability of the sub-cell FDTD algorithm because it is derived from an intensity equation and not from the full set of discrete equations. Therefore, we derive a new stability condition based on the Von Neuman analysis of the discrete system of equations.

To this end, the discrete time-dependent field variables are Fourier transformed into the spatial spectral domain with the wavenumbers $\tilde{k}_x, \tilde{k}_y$, and $\tilde{k}_z$ in the x-, y-, and z-directions, respectively. The systems of equations can then be written in matrix form as

$$\mathbf{V}^{n+1} = \mathbf{G}\mathbf{V}^n \tag{17}$$

with the vector of field variables

$$\mathbf{V}^n = \left[\tilde{D}_x^{n+\frac{1}{2}}, \tilde{D}_y^{n+\frac{1}{2}}, \tilde{D}_z^{n+\frac{1}{2}}, \tilde{Q}^{n+\frac{1}{2}}, \tilde{H}_x^n, \tilde{H}_y^n, \tilde{H}_z^n, \tilde{I}_z^n\right]^T \tag{18}$$

and the growth matrix $\mathbf{G}$, given in (19), shown at the bottom of the following page, where

$$W_i = 2\frac{c_0\Delta t\Delta i}{\sin}\left(\frac{\tilde{k}_i\Delta i}{2}\right)\ldots, \qquad i = x, y, z \tag{20}$$

$$L^{\triangle} = \frac{c_0\Delta t}{L} \tag{21}$$

$$P^{\triangle} = \frac{c_0\Delta t}{\Delta x\Delta y}. \tag{22}$$

The eigenvalues of the growth matrix are obtained using the symbolic mathematics software MAPLE. According to the

Von Neuman stability criterion, an algorithm is stable if the magnitude of all eigenvalues of the growth matrix remain less than or equal to one [13]. Assuming that a wire in the sub-cell model is oriented in the z-direction, we find that the limit on the eigenvalues yields two constraints on the maximum stable time step

$$\Delta t_{\max,\mathrm{CFL}} = \frac{1}{c_0\sqrt{\frac{1}{\Delta x^2}+\frac{1}{\Delta y^2}+\frac{1}{\Delta z^2}}} \tag{23}$$

and

$$\Delta t_{\max,\mathrm{TS}} = \frac{1}{c_0\sqrt{\frac{1}{\Delta x^2}+\frac{1}{\Delta y^2}+\frac{1}{\Delta z^2}+\frac{1}{4L\Delta x\Delta y}}} \tag{24}$$

where $\Delta t_{\max,\mathrm{CFL}}$ is the same CFL stability limit that exists for Yee's FDTD method and $\Delta t_{\max,\mathrm{TS}}$ is the maximum time step for the thin-strut FDTD method. It can easily be shown that $\Delta t_{\max,\mathrm{TS}} \leq \Delta t_{\max,\mathrm{CFL}}$ for all L. Consequently, the maximum time step is always smaller than the CFL limit, and (24) should be used to determine the maximum usable time step for the thin-strut algorithm. Since the time-step limit is a function of the in-cell inductance L of the wire model, it is directly dependent on the radius r_0 of an embedded wire. To gain insight into how the maximum stable time step is reduced by the introduction of a wire model, we normalize using the CFL limit assuming a uniform grid $\Delta x = \Delta y = \Delta z = h$ and obtain

$$\frac{\Delta t_{\max,\mathrm{TS}}}{\Delta t_{\max,\mathrm{CFL}}} = \sqrt{\frac{12L}{12L+1}} \leq 1. \tag{25}$$

Fig. 1 shows the newly derived maximum stable time step for the thin-strut FDTD method $(\Delta t_{\max,\mathrm{TS}})$, which is normalized using the CFL limit $(\Delta t_{\max,\mathrm{CFL}})$ as a function of the wire radius (r_0), which is normalized using the FDTD cell size (h). This figure also indicates the stability or instability of thin-strut simulations that were run using a range of different time step lengths and wire radii. For the numerical simulations, a sinusoidal source function with frequency $f = 2$ MHz was used. The mesh resolution was constant and uniform with $h = 3.4$ mm, corresponding to the CFL limit $\Delta t_{\max,\mathrm{CFL}} = 6.55$ ps. The time-step lengths were varied in the range $\Delta t/\Delta t_{\max,\mathrm{CFL}} = 0.1,\ldots,1$. The model consisted of a center-fed thin-strut dipole, 20 cells long with variable wire radius $r_0/h = 0,\ldots,0.5$. The computational space was terminated with a perfectly matched layer (PML), 12 cells wide, at distance of 15 cells away from the dipole, which corresponds to a total simulation size of 55, 55, and 74 cells in the x-, y-, and z-directions, respectively.

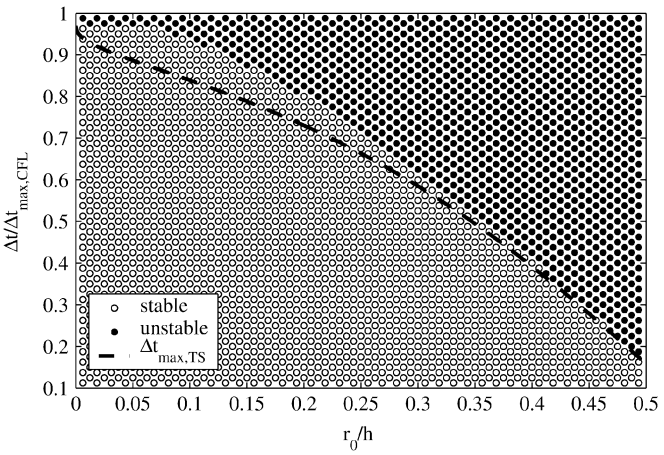

Fig. 1. Derived sufficient condition for stability (dotted line) and stability of the thin-strut method. Solid dots: unstable experiments. Circles: stable experiments.

Fig. 1 displays good agreement between the newly derived stability limit and the stability of our range of test simulations. This figure also illustrates that the maximum usable time-step for the thin-strut FDTD method is reduced as an in-cell inductance is entered into the wire model. In turn, there exists a practical limit to the largest wire radius that can be modeled by the thin-strut FDTD method because the maximum time step quickly approaches zero as the wire radius becomes half the cell size.

Further, we note that there is a small discrepancy between the derived stability bound and the actual stability limit observed in the numerical experiments. We attribute this to a property of the von Neuman stability condition, which is that it is a sufficient, but not necessary condition for stability unless the growth matrix is normal [14]; therefore, the maximum stable time step of the von Neuman condition can be below the stability bound observed in experiments. Thus, it has been shown experimentally that the time step given in (24) is indeed a sufficient condition for the stability of the thin-strut FDTD method.

III. Numerical Results

A. Coil Coupling

The coupling of two parallel concentric square coils, as illustrated in Fig. 2, was calculated using the thin-strut FDTD

$$\mathbf{G} = \left[\begin{array}{ccc|c|ccc|c}
1 & 0 & 0 & 0 & 0 & jW_z & -jW_y & 0 \\
0 & 1 & 0 & 0 & -jW_z & 0 & jW_x & 0 \\
0 & 0 & 1 & 0 & jW_y & -jW_x & 0 & -P^{\triangle} \\
\hline
0 & 0 & 0 & 1 & 0 & 0 & 0 & jW_z \\
\hline
0 & -jW_z & jW_y & 0 & 1-W_y^2-W_z^2 & W_xW_y & W_xW_z & -jW_yP^{\triangle} \\
jW_z & 0 & -jW_x & 0 & W_xW_y & 1-W_x^2-W_z^2 & W_yW_z & jW_xP^{\triangle} \\
-jW_y & jW_x & 0 & 0 & W_xW_z & W_yW_z & 1-W_x^2-W_y^2 & 0 \\
\hline
0 & 0 & L^{\triangle} & jW_z & jW_yL^{\triangle} & -jW_xL^{\triangle} & 0 & 1-W_z^2-L^{\triangle}P^{\triangle}
\end{array}\right] \tag{19}$$

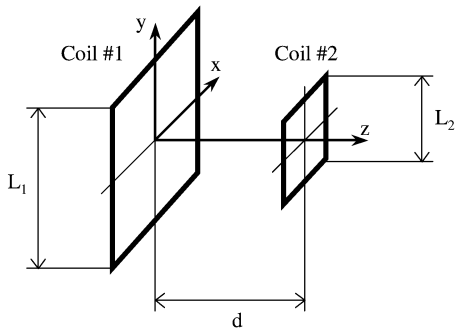

Fig. 2. Illustration of the problem geometry: two parallel concentric square coils.

method and the conventional FDTD method. Since currents are easily observable in the FDTD method, the ratio of currents in the primary source coil I_1 and the secondary receiving coil I_2 was used as a figure-of-merit for the coupling efficiency. The constitutive relations for the currents in two lossless mutually coupled closed conductor loops can be written as

$$\begin{pmatrix} L_1 & M_{12} \\ M_{12} & L_2 \end{pmatrix} \cdot \frac{\partial}{\partial t} \begin{pmatrix} I_1 \\ I_2 \end{pmatrix} = 0 \tag{26}$$

where M_{12} is the mutual inductance and L_1 and L_2 are the coil self-inductances, respectively. For sinusoidal signals, the current ratio can then be written as

$$\left|\frac{I_2}{I_1}\right| \equiv \frac{\partial}{\partial t}\left|\frac{I_2}{I_1}\right| = \left|\frac{M_{12}}{L_2}\right| = \left|\frac{L_1}{M_{12}}\right|. \tag{27}$$

In turn, for low frequencies, the inductance values and current ratios for simple coil geometries can be approximated using the Biot–Savart law, which served as our analytical approximation for the verification of the FDTD results.

B. FDTD Simulations

In the FDTD computations, a current I_1 was excited in the primary coil by updating the corresponding H-field components around the wire according to the sinusoidal source function with frequency $f = 2$ MHz. Similarly, the current I_2 coupled into the secondary coil was observed from the H-field around the wire. The current amplitudes in the source and secondary coils were calculated by a least squares curve fit of the FDTD data to a sinusoidal function.

The lengths of the sides of the primary coil were varied in the range $s_1 = 5, \ldots, 85$ mm. The distance between the coils was varied in the range $d = 0, \ldots, 40$ mm. The length of the sides of the secondary coil was $s_2 = 6$ mm in all cases. Mesh resolutions of 1.0 and 0.5 mm were used. The computational space was terminated with a PML, 16 cells wide, at a distance of 20 cells away from the coils. To reduce the run time of the numerical computations, the simulations were terminated after a quarter period. The wire radius that was used for the thin-strut wire model was $r_0 = 0.025$ mm.

Fig. 3 shows results obtained from the thin-strut FDTD and the conventional FDTD methods compared to the analytical approximation. The graph shows the current ratio as a function of the coil distance where the size of the primary coil was $s_1 = 50$ mm. Similarly, Fig. 4 shows the current ratios for the two methods as the coil size s_1 is varied for a fixed coil distance $d = 20$ mm. As both graphs show, the thin-strut FDTD method is in better agreement with the analytical approximation than the conventional FDTD method.

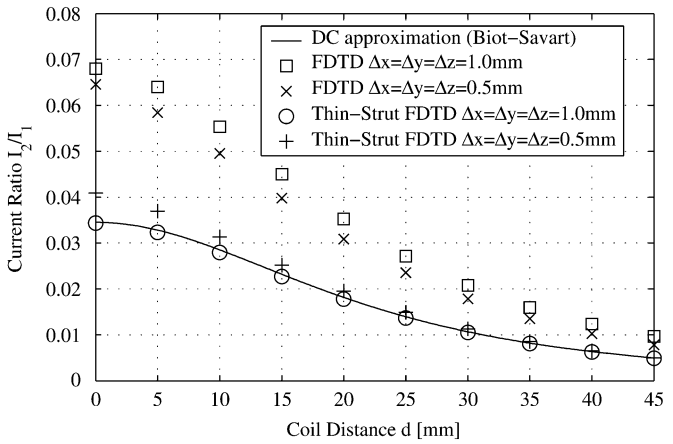

Fig. 3. Ratio of currents in the primary and secondary coils as a function of coil distance obtained from the FDTD method, the thin-strut FDTD method, and an analytical approximation ($s_1 = 50$ mm).

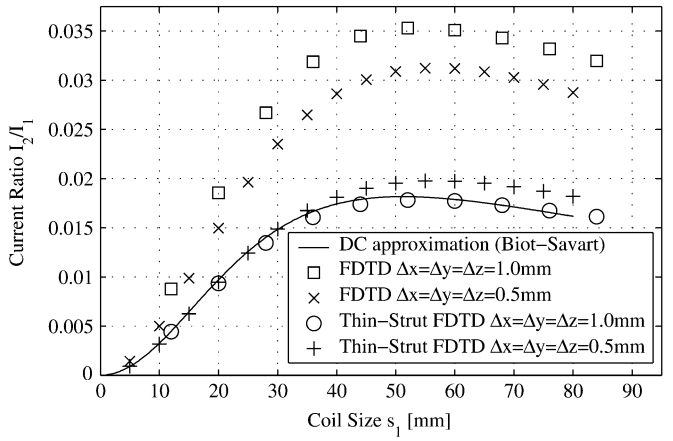

Fig. 4. Ratio of currents in the primary and secondary coils as a function of the size of the primary coil obtained from the FDTD method, the thin-strut FDTD method, and an analytical approximation ($d = 20$ mm).

IV. Conclusion

A new stability condition based on a Von Neuman stability analysis has been derived for the thin-strut FDTD method. The newly derived stability bound has been verified experimentally and has proven to be a sufficient condition for stability. The maximum stable time step is a function of the in-cell inductance used in the thin-wire model. This stability bound limits the utility of the thin-strut method to wire radii that are less than half the cell size of the FDTD mesh.

The thin-strut FDTD method was used to calculate the current coupling between a primary source coil and a smaller coaxial secondary coil as a function of the coil separation and coil size. The results were compared to those obtained from the conventional FDTD method and an analytical approximation. Results indicate that the thin-strut formalism can model wire structures more accurately than the conventional FDTD method. Thus, the

thin-strut method appears to be promising for the study and design of coils for telemetry links between implantable and external devices. Further, the implementation used here can be extended to include frequency-dispersive materials to more accurately describe tissue models used in computations for biomedical telemetry applications.

ACKNOWLEDGMENT

The authors gratefully acknowledge Y. Liu for her preliminary work, which led to this study.

REFERENCES

[1] K. Finkenzeller, *RFID Handbook: Fundamentals and Applications in Contactless Smart Cards and Identification*, 2nd ed. Hoboken, NJ: Wiley, 2003.

[2] N. D.-N. Donaldson and T. A. Perkins, "Analysis of resonant coupled coils in the design of radio frequency transcutaneous links," *Med. Biol. Eng. Comput.*, vol. 21, no. 5, pp. 612–27, 1983.

[3] F. C. Flack, E. D. James, and D. M. Schlapp, "Mutual inductance of air-cored coils: Effect on design of radio-frequency coupled implants," *Med. Biol. Eng.*, vol. 9, no. 2, pp. 79–85, 1971.

[4] D. C. Galbraith, M. Soma, and R. L. White, "A wide-band efficient inductive transdermal power and data link with coupling insensitive gain," *IEEE Trans. Biomed. Eng.*, vol. BME-34, pp. 265–275, Apr. 1987.

[5] C. R. Neagu, H. V. Jansen, A. Smith, J. G. E. Gardeniers, and M. C. Elwenspoek, "Characterization of a planar microcoil for implantable microsystems," *Sens. Actuators A, Phys.*, vol. A62, no. 1–3, pp. 599–611, 1997.

[6] M. Soma, D. C. Galbraith, and R. L. White, "Radio-frequency coils in implantable devices: Misalignment analysis and design procedure," *IEEE Trans. Biomed. Eng.*, vol. BME-34, pp. 276–282, Apr. 1987.

[7] C. Zierhofer and E. Hochmair, "Geometric approach for coupling enhancement of magnetically coupled coils," *IEEE Trans. Biomed. Eng.*, vol. 43, pp. 708–714, July 1996.

[8] O. Mohammed, W. Batina, and L. Gipson, "Electromagnetic field modeling of implantable telemetry systems," *IEEE Trans. Magn.*, vol. MAG-21, pp. 2068–2070, May 1985.

[9] A. Taflove and S. C. Hagness, *Computational Electrodynamics: The Finite-Difference Time-Domain Method*, 2nd ed. Boston, MA: Artech House, 2000.

[10] R. Holland and L. Simpson, "Finite-difference analysis of EMP coupling to thin struts and wires," *IEEE Trans. Electromagn. Compat.*, vol. EMC-23, pp. 88–97, May 1981.

[11] D. Sullivan, "An unsplit step 3-d PML for use with the FDTD method," *IEEE Microwave Guided Wave Lett.*, vol. 7, pp. 184–186, July 1997.

[12] J. Grando, F. Issac, M. Lemistre, and J. Alliot, "Stability analysis including wires of arbitrary radius in FD-TD code," in *IEEE AP-S Int. Symp. Dig.*, vol. 1, 1993, pp. 18–21.

[13] G. D. Smith, *Numerical Solution of Partial Differential Equations: Finite Difference Methods*, 3rd ed. New York: Oxford Univ. Press, 1985.

[14] R. D. Richtmyer and K. W. Morton, *Difference Methods for Initial-Value Problems*, 2nd ed. New York: Interscience, 1967.

Stefan Schmidt (S'02) was born in Peine, Germany, in 1974. He studied electrical engineering at the Technische Universität Braunschweig, Braunschweig, Germany until 1998. He received the M.S. degree in electrical engineering from the University of Kentucky, Lexington, in 2000, and is currently working toward the Ph.D. degree at North Carolina State University, Raleigh.

His research interests include remote query sensors, magnetic materials, computational electromagnetics, and bioelectromagnetics.

Mr. Schmidt is a member of Eta Kappa Nu.

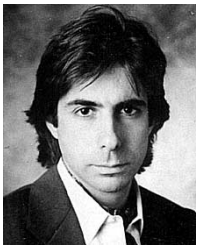

Gianluca Lazzi (S'94–M'95–SM'99) was born in Rome, Italy, on April 25, 1970. He received the Dr.Eng. degree in electronics from the University of Rome "La Sapienza," Rome, Italy, in 1994, and the Ph.D. degree in electrical engineering from the University of Utah, Salt Lake City, in 1998.

He has been a consultant for several companies (1988–1994), a Visiting Researcher with the Italian National Board for New Technologies, Energy, and Environment (ENEA) (1994), a Visiting Researcher with the University of Rome "La Sapienza" (1994–1995), and a Research Associate (1995–1998) and Research Assistant Professor (1998–1999) with the University of Utah. He is currently an Associate Professor with the Department of Electrical and Computer Engineering, North Carolina State University (NCSU), Raleigh, where, from 1999 to 2003, he was an Assistant Professor. He has authored or coauthored over 80 international journal papers or conference presentations on FDTD modeling, dosimetry, and bioelectromagnetics. He is listed in *Who's Who in the World*, *Who's Who in America*, *Who's Who in Science and Engineering*, the *Dictionary of International Biographies*, and the 2000 *Outstanding Scientists of the 20th Century*.

Dr. Lazzi is an associate editor for the *IEEE Antennas and Wireless Propagation Letters*. He is the vice chair of Commission K (Electromagnetics in Biology and Medicine), U.S. National Committee of the International Union of Radio Science (URSI). He was the recipient of the 2003 ALCOA Foundation Engineering Research Achievement Award, a 2003 NCSU Outstanding Teacher Award, the 2003 NCSU Alumni Outstanding Teacher Award, a 2001 National Science Foundation (NSF) CAREER Award, a 2001 Whitaker Foundation Biomedical Engineering Grant for Young Investigators, a 1996 International Union of Radio Science (URSI) Young Scientist Award, and the 1996 Curtis Carl Johnson Memorial Award for the best student paper presented at the 18th Annual Technical Meeting of the IEEE Bioelectromagnetics Society (IEEE BEMS).